Acta Cryst E CRYSTALLOGRAPHIC COMMUNICATIONS

ISSN 2056-9890

Synthesis, crystal structure and Hirshfeld surface analysis of *N*-(2,6-dimethylphenyl)-2-morpholino-acetamide, a Lidocaine analog

Imane Maimoune,[a,b] Abderrazzak El Moutaouakil Ala Allah,[a] Benson M. Kariuki,[c] Abdulsalam Alsubari,[d]* Joel T. Mague,[e] Abdelkader Zarrouk[b] and Youssef Ramli[a]*

[a]Laboratory of Medicinal Chemistry, Drug Sciences Research Center, Faculty of Medicine and Pharmacy Mohammed V University in Rabat, Morocco, [b]Laboratory of Materials Nanotechnology and Environment, Faculty of Sciences, Mohammed V University in Rabat, PO Box 1014, Rabat, Morocco, [c]School of Chemistry, Cardiff University, Main Building Park Place, Cardiff, CF10 3AT, United Kingdom, [d]Laboratory of Medicinal Chemistry, Faculty of Clinical Pharmacy, 21 September University, Yemen, and [e]Department of Chemistry, Tulane University New Orleans, LA, 70118, USA. *Correspondence e-mail: alsubaripharmaco@21umas.edu.ye, y.ramli@um5r.ac.ma

Received 11 May 2026
Accepted 8 June 2026

Edited by J. Ellena, Universidade de São Paulo, Brazil

Keywords: crystal structure; acetamide; hydrogen bond; morpholine; Lidocaine; Hirshfeld surface.

CCDC reference: 2560706

Supporting information: this article has supporting information at journals.iucr.org/e

In the title molecule, $C_{14}H_{20}N_2O_2$, the dihedral angle between the mean plane of the phenyl ring and that defined by the *ipso*-C—NH—(C═O)—CH_2— unit is 66.59 (11)°. The morpholine unit adopts a chair conformation. In the crystal, N—H···O hydrogen bonds and C—H···π(ring) interactions form chains extending along the *b*-axis direction. A Hirshfeld surface analysis showed H···H contacts to constitute nearly 70% of the intermolecular contacts in the crystal.

1. Chemical context

In medicinal chemistry, heterocyclic compounds, particularly those with a nitrogen atom, are crucial, forming the core of over 90% of new drugs and vital biomolecules such as vitamins and DNA (Al Mulla, 2017). Numerous studies on the acetamide family have shown that it can be found in a variety of well-known medications from different classes with a range of therapeutic effects. They have a wide range of biological activities due to their structural resemblance to numerous bioactive natural and synthetic molecules (Missioui *et al.*, 2022*a*). A heterocyclic substance with local anesthetic properties is lidocaine. It is composed of a hydrophilic amine and a lipophilic aromatic ring. Its primary target in excitable cells is the voltage-gated sodium channel, which causes the elevated sodium permeability seen in skeletal muscles, peripheral nerves, neuroendocrine, and cardiac cells during the rising phase of the action potential.

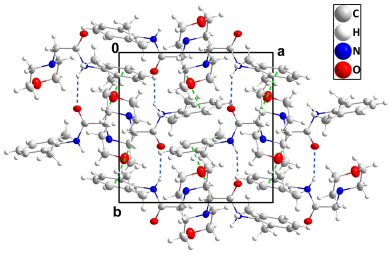

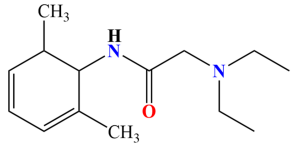

Lidocaine

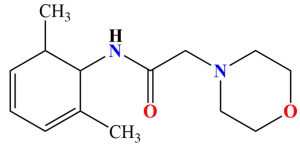

3

As part of our research in this field (Maimoune *et al.*, 2025), we synthesized the lidocaine analogue *N*-(2,6-dimethylphen-

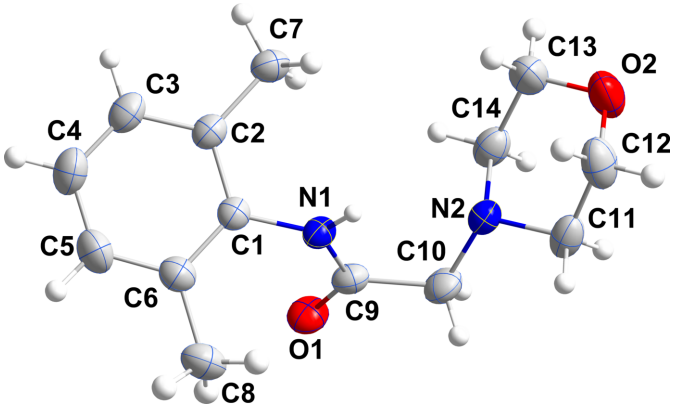

Figure 1
Perspective view of the title molecule with the abeling scheme and 30% probability ellipsoids.

yl)-2-morpholinoacetamide, **3**, via an alkylation reaction of morpholine by 2-chloro-*N*-(2,6-dimethylphenyl)acetamide under refluxing toluene, the crystal structure of which is presented in this paper. The intermolecular interactions were examined using a Hirshfeld surface analysis.

2. Structural commentary

In the title molecule **3**, Fig. 1, the dihedral angle between the mean plane of the C1–C6 ring and the plane defined by atoms C1/N1/C9/C10 is 66.59 (11)° while the dihedral angle between the latter plane and that defined by atoms C11–C14 is 63.59 (11)°. The morpholine unit adopts a chair conformation. Bond lengths and interbond angles are as expected. An intramolecular N—H···N contact is observed (Table 1).

3. Supramolecular features

In the crystal, N1—H1···O1^{i} hydrogen bonds and C10—H10*B*···*Cg*2^{ii} interactions (Table 1) form chains extending along the *b*-axis direction (Fig. 2). The chains largely pack with normal van der Waals contacts.

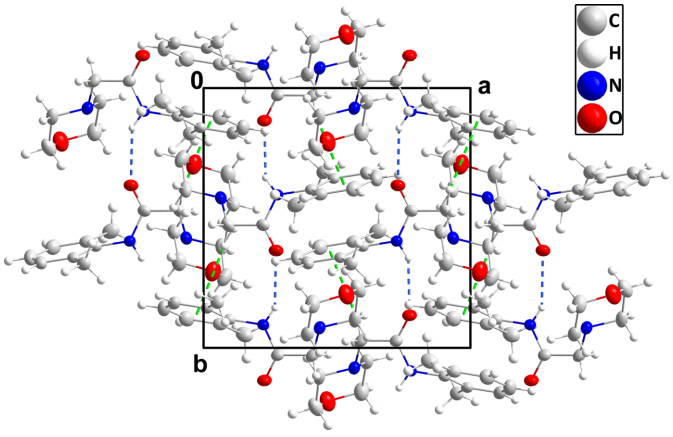

Figure 2
Packing viewed along the *c*-axis direction with N—H···O hydrogen bonds and C—H···π(ring) interactions depicted, respectively, by blue and green dashed lines.

Table 1
Hydrogen-bond geometry (Å, °).

*Cg*2 is the centroid of the C1–C6 ring.

D—H···*A*	*D*—H	H···*A*	*D*···*A*	*D*—H···*A*
N1—H1···N2	0.88 (2)	2.278 (18)	2.738 (2)	112.5 (16)
N1—H1···O1^{i}	0.88 (2)	2.34 (2)	3.0798 (18)	141.3 (16)
C10—H10*B*···*Cg*2^{ii}	0.97	2.94	3.782 (2)	146

Symmetry codes: (i) $-x+\frac{3}{2}, y+\frac{1}{2}, -z+\frac{3}{2}$; (ii) $-x+\frac{3}{2}, y-\frac{1}{2}, -z+\frac{3}{2}$.

4. Database survey

A search of the Cambridge Structural Database (CSD, updated to April 2026; Groom, *et al.*, 2016) with the fragment pictured in Fig. 3 (*R* = N) gave 99 hits, many of which were either metal complexes or salts in which $R = R'R''NH^{+}$ (R' and R'' = alkyl groups). Excluding these, 36 hits remained that were considered similar to the title molecule and of these, 25 were co-crystals (Table 2 with *R* defined in Fig. 3). One of the more salient quantities common to all, and the most likely to vary, is the dihedral angle between the mean plane of the 2,6-dimethylphenyl ring and the plane defined by the *ipso*-C—NH—(C═O)—CH_2— unit. This is likely to be large to avoid close contacts between the methyl and carbonyl groups. Indeed, the smallest value is 57.2 (2)° in CINBEK but can be as large as 86.4 (3)° in WEDXAH, although the majority are in the range 60–75° as is the case for **3**. Considering those that are not co-crystals, this angle has a range of 57.2 (2)° (in CINBEK) to 82.0° (in LIDCAN10) and since the *R* group is fairly remote from the *ipso*-C—N bond, the variation is likely due to packing considerations. A comparable range for the dihedral angle is also seen in the co-crystals and there does not appear to be any definite correlation with the size of the second component.

5. Hirshfeld surface analysis

The Hirshfeld surface of **3** was calculated with *CrystalExplorer17* (Spackman *et al.*, 2021) and mapped over d_{norm} from −0.1546 to 1.1576 in arbitrary units. It is shown, together with two neighboring molecules and the hydrogen bonds between them, in Fig. 4. Details of the appearance and interpretations of the plots generated by *CrystalExplorer* have

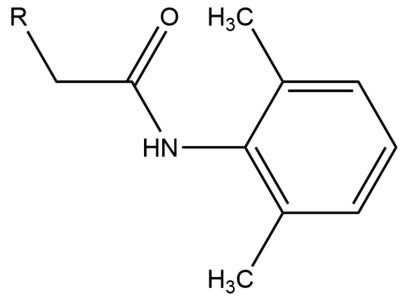

Figure 3
The search fragment used for the *Database survey*.

Table 2
Database Survey.

REFCODE	*R*	Component 2	Dihedral angle (°)	Reference
BIDVET	NEt_2	2-*i*-propyl-5-methylcyclohexanol	85.4 (13)	Ma *et al.* (2023)
BIDVET01	NEt_2	2-*i*-propyl-5-methylcyclohexanol	85.6 (14)	Ma *et al.* (2023)
BIDVET02	NEt_2	2-*i*-propyl-5-methylcyclohexanol	84.4 (6)	Ma *et al.* (2023)
DALJIN	NEt_2	nonanedioic acid	58.90 (15), 65.00 (15)	Zotova *et al.* (2021)
LIDCAN10	NEt_2	–	82.0, 77.8	Hanson & Banner (1974)
LIDCAN11	NEt_2	–	76.0 (6), 75.6 (6)	Bambagiotti-Alberti *et al.* (2007)
LIDCAN12	NEt_2	–	79.79 (15), 72.74 (10), 68.41 (16), 78.93 (16)	Gryl (2015)
SEQRAJ	NEt_2	2-*i*-propyl-5-methylcyclohexanol	76.05 (18)	Corvis *et al.* (2010)
TURNOW	NEt_2	1,3,5-trihydroxybenzene	71.24 (8)	Magaña-Vergara *et al.* (2018)
WEDWUA	NEt_2	1,4-dibromo-2,3,5,6-tetrafluorobenzene	78.42 (17)	Choquesillo-Lazarte *et al.* (2017)
WEDXAH	NEt_2	1,4-diiodo-2,3,5,6-tetrafluorobenzene	86.4 (3)	Choquesillo-Lazarte *et al.* (2017)
GENRAT	pyrrolidin-2-one-1-yl	–	66.49 (15)	Wang *et al.* (2006*b*)
KAJSIB	pyrrolidin-2-one-1-yl	2-hydroxy-2-phenylacetic acid	60.87 (16)	Buol *et al.* (2020*a*)
KAJSIB01	pyrrolidin-2-one-1-yl	2-hydroxy-2-phenylacetic acid	60.84 (14)	Buol *et al.* (2020*a*)
OYUWOX	pyrrolidin-2-one-1-yl	2-phenylsuccinic acid	61.23 (18)	Buol *et al.* (2020*a*)
OYUWUD01	pyrrolidin-2-one-1-yl	5-nitroisophthalic acid	71.59 (13)	Buol *et al.* (2020*a*)
OYUXAK	pyrrolidin-2-one-1-yl	4-hydroxybenzoic acid	64.89 (12)	Buol *et al.* (2020*b*)
OYUXIS	pyrrolidin-2-one-1-yl	5-cyanoisophthalic acid	68.75 (19)	Buol *et al.* (2020*b*)
OYUXOY	pyrrolidin-2-one-1-yl	2-benzoylbenzoic acid	60.03 (17)	Buol *et al.* (2020*b*)
OYUXUE	pyrrolidin-2-one-1-yl	2-hydroxy-3-phenylpropanoic acid	60.4 (2)	Buol *et al.* (2020*b*)
OYUYAL	pyrrolidin-2-one-1-yl	2-phenylbutyric acid	61.6 (8)	Buol *et al.* (2020*b*)
OYUYEP	pyrrolidin-2-one-1-yl	5-hydroxyisophthalic acid	74.91 (9), 78.08 (9)	Buol *et al.* (2020*a*)
OYUYIT	pyrrolidin-2-one-1-yl	2-hydroxypropane-1,2,3-tricarboxylic acid	69 (9)	Buol *et al.* (2020*a*)
OYUYIT01	pyrrolidin-2-one-1-yl	2-hydroxypropane-1,2,3-tricarboxylic acid	69.7 (9), 69.0 (9), 67.7 (7), 70.5 (8)	Buol *et al.* (2020*b*)
OYUZAM	pyrrolidin-2-one-1-yl	oxalic acid	69.6 (6), 67.0 (7), 68.9 (8), 77.0 (8)	Buol *et al.* (2020*a*)
OYUZOA	pyrrolidin-2-one-1-yl	3,4,5-trihydroxybenzoic acid	70.4 (7), 72.1 (9)	Buol *et al.* (2020*b*)
ACEZAK	4-*R*′-piperazin-1-yl[a]	–	64.23 (19)	Wang *et al.* (2004)
CINBEK	4-*R*′-piperazin-1-yl[b]	–	57.2 (2)	Silva *et al.* (2023)
JAYSAE	4-*R*′-piperazin-1-yl[c]	–	67.73 (16)	Wang *et al.* (2005*b*)
LIPFAZ	4-*R*''-piperazin-1-yl[d]	–	73.3 (4)	Germain *et al.* (1977)
MAPKIY	4-*R*′-piperazin-1-yl[e]	–	63.86 (17)	Wang *et al.* (2005*a*)
SENCAQ	4-*R*′-piperazin-1-yl[f]	–	65.5 (6)	Wang *et al.* (2006*a*)
SEJLOM	3-hydroxy-3-methoxymethyl-2-oxoindolin-1-yl	–	72.76 (8)	Nchioua *et al.* (2022)
VAVGIM	4-(2,6-dimethylphenyl)-3,5-dioxopiperazin-1-yl	–	73.98 (15)	Heim *et al.* (2021)
YOTROO	$N(CH_2COOH)_2$	–	60.88 (18)	Ribár *et al.* (1995)
YOTRUU	$N(CH_2COOH)[CH_2C(O)OMe]$	–	74.5 (4)	Ribár *et al.* (1995)

Notes: (*a*) *R*′ = 3-(4-nitrophenyl)-1,2,4-oxadiazol-5-ylmethyl; (*b*) *R*′ = 2-hydroxy-3-(2-methoxyphenoxy)propyl; (*c*) *R*′ = 3-(3-methoxyphenyl)-1,2,4-oxadiazol-5-ylmethyl; (*d*) *R*′ = 4,4-bis(4-fluorophenyl)butyl; (*e*) *R*′ = 3-(2-chlorophenyl)-1,2,4-oxadiazol-5-ylmethyl; (*f*) *R*′ = 3-(4-bromophenyl)-1,2,4-oxadiazol-5-ylmethyl.

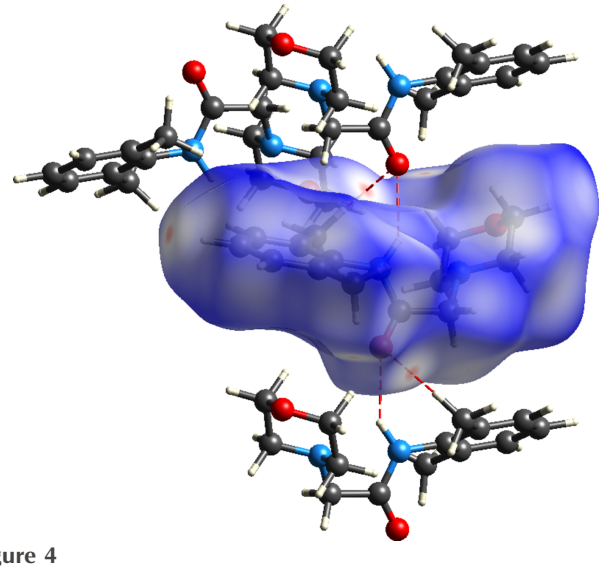

Figure 4
The d_{norm} Hirshfeld surface of the title molecule with two neighboring molecules in the hydrogen-bonded chain. The N—H···O hydrogen bonds are shown as dashed lines.

been published (Tan *et al.*, 2019). The ensemble in Fig. 4 is a portion of the hydrogen-bonded chain depicted in Fig. 2. Fig. 5 presents the fingerprint plots showing all intermolecular contacts (5*a*) and those showing each of the three most significant ones. The H···H contacts (5*b*) comprise 69.2% of the total, consistent with the periphery of the molecule being largely hydrogen atoms. The next most important are the O···H/H···O contacts at 16.7% of the total (5*c*), which appear as a pair of sharp spikes at $d_e + d_i \simeq 2.3$ Å with broad shoulders at $d_e + d_i \simeq 2.6$ Å: the former represent the N1—H1···O1^{i} hydrogen bonds (Table 1) while the latter are attributed to C—H···O contacts, which range from 2.66 to 2.73 Å and are considered to be slightly compressed van der Waals contacts rather than significant C—H···O hydrogen bonds. The last are the C···H/H···C contacts (5***d***) appearing as a pair of broad peaks at $d_e + d_i \simeq 2.8$ Å and attributed, in part, to the C—H···π(ring) interactions listed in Table 1 and contributing 14.0% to the total. The results of this analysis show a strong, 1-D supramolecular component to the crystal but relatively weak interactions in the other two directions.

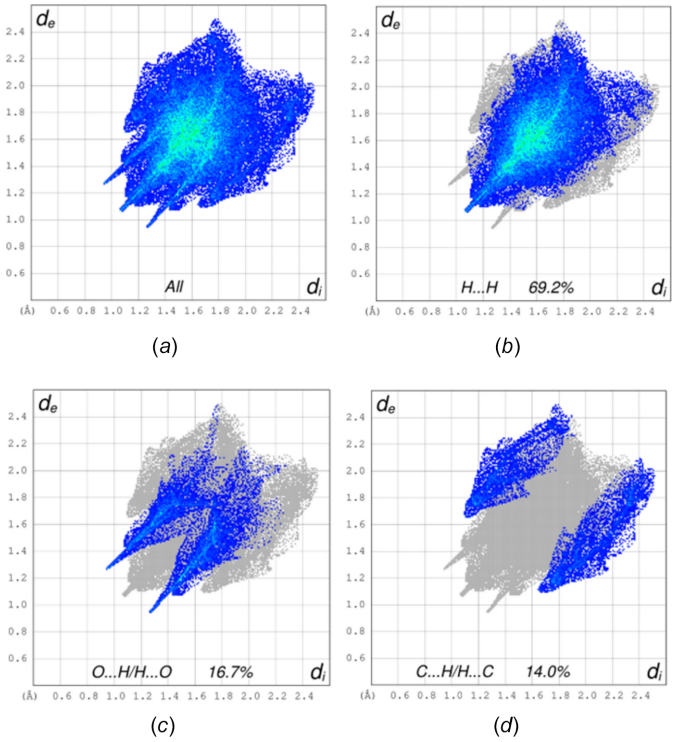

Figure 5
The two-dimensional fingerprint plots for the title molecule showing (*a*) all contacts, (*b*) H···H contacts, (*c*) O···H/H···O contacts and (*d*) C···H/H···C contacts.

6. Synthesis and crystallization

The reaction sequence for preparing **3** is shown in Fig. 6. 2-Chloro-*N*-(2,6-dimethylphenyl)acetamide, **1**, was synthesized according to the procedure described in the literature (Missioui *et al.*, 2022*b*). Next, 1.2 mmol of morpholine, **2**, were mixed with 1 mmol of 2-chloro-*N*-(4-nitrophenyl)acetamide and refluxed in toluene for 4 h. Upon completion of the reaction, toluene was removed by liquid–liquid extraction, and the aqueous phase was subsequently acidified with hydrochloric acid to adjust its pH to about 4, prompting the precipitation of **3**. The precipitate was filtered off, dried, and recrystallized from ethanol solution, yielding white crystals.

Yield = 45%, color: white, m.p. = 399–401 K. **FT–IR** (ATR, cm^{-1}) : 3228 (N—H amide), 2956 (C—H aliphatic), 1661(C═O). **^{1}H NMR** (500 MHz, DMSO-d_6) δ(ppm): 2.10 (*s*, 6 H, CH_3), 2.5 (*t*, 4 H, N—CH_2—C), 3.09 (*s*, 2 H, CH_2 amide), 3.62 (*t*, 4 H, O—CH_2—C), 7.02–7.04 (*m*, 3 H, H_{ar}), and 9.20 (*s*, 1 H, NH amide). **^{13}C NMR** (125 MHz, DMSO-d_6) δ(ppm): 18.76 (CH_3), 53.97 (N—CH_2—C), 62.15 (N—CH_2—C—O), 66.62 (O—CH_2—C), 126.94, 128.20, 135.59, 135.74 (C_ar), and 168.34 (C═O). **HRMS (ESI):** calculated for $C_{14}H_{20}N_2O_2$ [M + H]$^+$ 249.1525; found 249.15874.

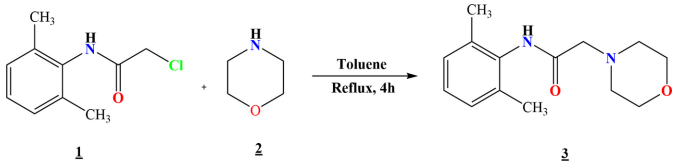

Figure 6
Reaction scheme for the formation of the title compound **3**.

Table 3
Experimental details.

Crystal data	
Chemical formula	$C_{14}H_{20}N_2O_2$
M_r	248.32
Crystal system, space group	Monoclinic, $P2_1/n$
Temperature (K)	293
a, b, c (Å)	12.2417 (9), 10.4498 (4), 12.2866 (9)
β (°)	118.704 (9)
V (Å^3)	1378.59 (18)
Z	4
Radiation type	Cu $K\alpha$
μ (mm^{-1})	0.65
Crystal size (mm)	0.49 × 0.23 × 0.14
Data collection	
Diffractometer	SuperNova, Dual, Cu at home/near, Atlas
Absorption correction	Gaussian (*CrysAlis PRO*; Rigaku OD, 2024)
T_{min}, T_{max}	0.326, 1.000
No. of measured, independent and observed [$I > 2\sigma(I)$] reflections	9760, 2709, 1991
R_{int}	0.028
(sin $\theta/\lambda)_{max}$ (Å^{-1})	0.620
Refinement	
$R[F^2 > 2\sigma(F^2)]$, $wR(F^2)$, S	0.046, 0.142, 1.04
No. of reflections	2709
No. of parameters	169
No. of restraints	1
H-atom treatment	H atoms treated by a mixture of independent and constrained refinement
$\Delta\rho_{max}$, $\Delta\rho_{min}$ (e Å^{-3})	0.15, −0.18

Computer programs: *CrysAlis PRO* (Rigaku OD, 2024), *SHELXT* (Sheldrick, 2015*a*), *SHELXL* (Sheldrick, 2015*b*) and , *DIAMOND* (Brandenburg & Putz, 2012).

7. Refinement

Crystal data, data collection and structure refinement details are summarized in Table 3. The N—H H atom was refined freely. C-bound H atoms were positioned with idealized geometry (C—H = 0.93–0.97 Å) and refined using a riding model with U_{iso}(H) = 1.2 or 1.5U_{eq}(C).

Acknowledgements

YR is thankful to the National Center for Scientific and Technical Research of Morocco (CNRST) for its continuous support. The contributions of the authors are as follows: conceptualization, YR; methodology, AA; investigation, IM and AEMAA; writing (original draft), JTM and AEMAA; writing (review and editing of the manuscript), YR and BMK; formal analysis, YR and JTM; supervision, YR and AZ; crystal structure determination, BMK.

References

Al Mulla, A. (2017). *Der Pharma Chemica*. **9**, 141–147.

Bambagiotti-Alberti, M., Bruni, B., Di Vaira, M., Giannellini, V. & Guerri, A. (2007). *Acta Cryst.* E**63**, o768–o770.
Brandenburg, K. & Putz, H. (2012). *DIAMOND*. Crystal Impact GbR, Bonn, Germany.
Buol, X., Caro Garrido, C., Robeyns, K., Tumanov, N., Collard, L., Wouters, J. & Leyssens, T. (2020*a*). *Cryst. Growth Des.* **20**, 7979–7988.
Buol, X., Robeyns, K., Garrido, C. C., Tumanov, N., Collard, L., Wouters, J. & Leyssens, T. (2020*b*). *Pharmaceutics* **12**, 653-669.
Choquesillo-Lazarte, D., Nemec, V. & Cinčić, D. (2017). *CrystEngComm* **19**, 5293–5299.
Corvis, Y., Négrier, P., Lazerges, M., Massip, S., Léger, J.-M. & Espeau, P. (2010). *J. Phys. Chem. B* **114**, 5420–5426.
Germain, G., Declercq, J. P., Van Meerssche, M. & Koch, M. H. J. (1977). *Acta Cryst.* B**33**, 1971–1972.
Groom, C. R., Bruno, I. J., Lightfoot, M. P. & Ward, S. C. (2016). *Acta Cryst.* B**72**, 171–179.
Gryl, M. (2015). *Acta Cryst.* B**71**, 392–405.
Hanson, A. W. & Banner, D. W. (1974). *Acta Cryst.* B**30**, 2486–2488.
Heim, P., Twamley, B., O'Brien, J. & McDonald, A. R. (2021). *Chemistry Select* **6**, 9663-9668.
Ma, P., Toussaint, B., Roberti, E. A., Scornet, N., Silva, A. S., Henriquez, L. C., Cadasse, M., Negrier, P., Massip, S., Dufat, H., Hammad, K., Baraldi, C., Gamberini, M. C., Richard, C., Veesler, S., Espeau, P., Lee, T. & Corvis, Y. (2023). *Pharmaceutics* **15**, 1102-1126.
Magaña-Vergara, N., De la Cruz-Cruz, P., Peraza-Campos, A., Martínez-Martínez, F. & González-González, J. (2018). *Crystals* **8**, 130–138.
Maimoune, I., Kariuki, B. M., El Moutaouakil Ala Allah, A., Nchioua, I., Alsubari, A., Mague, J. T., Zarrouk, A. & Ramli, Y. (2025). *Acta Cryst.* E**81**, 69–73.
Missioui, M., Guerrab, W., Nchioua, I., El Moutaouakil Ala Allah, A., Kalonji Mubengayi, C., Alsubari, A., Mague, J. T. & Ramli, Y. (2022*b*). *Acta Cryst.* E**78**, 687–690.
Missioui, M., Mortada, S., Guerrab, W., Demirtaş, G., Mague, J. T., Ansar, M., El Abbes Faouzi, M., Essassi, E. M., Mehdar, Y. T. H., Aljohani, F. S., Said, M. & Ramli, Y. (2022*a*). *Arab. J. Chem.* **15**, 103851–103870.
Nchioua, I., Alsubari, A., Mague, J. T. & Ramli, Y. (2022). *Acta Cryst.* E**78**, 922–925.
Ribár, B., Mészáros, C., Vladimirov, S., Zivanov-Stakić, D., Jovanović, M., Zmbova, B. & Engel, P. (1995). *Struct. Chem.* **6**, 121–125.
Rigaku OD (2024). *CrysAlis PRO*. Rigaku Oxford Diffraction, Yarnton, England.
Sheldrick, G. M. (2015*a*). *Acta Cryst.* A**71**, 3–8.
Sheldrick, G. M. (2015*b*). *Acta Cryst.* C**71**, 3–8.
Silva, J. F. C., Pereira Silva, P. S., Ramos Silva, M., Fantechi, E., Chelazzi, L., Ciattini, S., Eusébio, M. & Rosado, M. T. S. (2023). *Cryst. Growth Des.* **23**, 6679–6691.
Spackman, P. R., Turner, M. J., McKinnon, J. J., Wolff, S. K., Grimwood, D. J., Jayatilaka, D. & Spackman, M. A. (2021). *J. Appl. Cryst.* **54**, 1006–1011.
Tan, S. L., Jotani, M. M. & Tiekink, E. R. T. (2019). *Acta Cryst.* E**75**, 308–318.
Wang, H.-B., Chen, J.-H., Pu, Y.-Q. & Wang, J.-T. (2004). *Acta Cryst.* E**60**, o2041–o2042.
Wang, H.-B., Liu, Z.-Q. & Yan, X.-C. (2006*a*). *Acta Cryst.* E**62**, o3465–o3466.
Wang, H.-B., Pu, Y.-Q., Chen, J.-H. & Wang, J.-T. (2005*a*). *Acta Cryst.* E**61**, o1994–o1996.
Wang, H.-B., Pu, Y.-Q., Chen, J.-H. & Wang, J.-T. (2005*b*). *Acta Cryst.* E**61**, o3750–o3751.
Wang, P.-L., Wang, H.-B., Ding, W.-L., Liu, Z.-Q. & Xing, Z.-T. (2006*b*). *Acta Cryst.* E**62**, o3838–o3839.
Zotova, J., Wojnarowska, Z., Twamley, B. & Tajber, L. (2021). *J. Mol. Liq.* **344**, 117737–117747.

supporting information

Acta Cryst. (2026). E**82**, 829-833 [https://doi.org/10.1107/S2056989026006043]

Synthesis, crystal structure and Hirshfeld surface analysis of *N*-(2,6-dimethylphenyl)-2-morpholinoacetamide, a Lidocaine analog

Imane Maimoune, Abderrazzak El Moutaouakil Ala Allah, Benson M. Kariuki, Abdulsalam Alsubari, Joel T. Mague, Abdelkader Zarrouk and Youssef Ramli

Computing details

N-(2,6-Dimethylphenyl)-2-(morpholin-4-yl)acetamide

Crystal data

$C_{14}H_{20}N_2O_2$
M_r = 248.32
Monoclinic, $P2_1/n$
a = 12.2417 (9) Å
b = 10.4498 (4) Å
c = 12.2866 (9) Å
β = 118.704 (9)°
V = 1378.59 (18) Å^3
Z = 4
$F(000)$ = 536
D_x = 1.196 Mg m^{-3}
Cu $K\alpha$ radiation, λ = 1.54184 Å
Cell parameters from 3200 reflections
θ = 4.2–72.3°
μ = 0.65 mm^{-1}
T = 293 K
Block, colourless
0.49 × 0.23 × 0.14 mm

Data collection

SuperNova, Dual, Cu at home/near, Atlas diffractometer
Detector resolution: 10.5082 pixels mm^{-1}
ω scans
Absorption correction: gaussian (CrysAlisPro; Rigaku OD, 2024)
T_{min} = 0.326, T_{max} = 1.000
9760 measured reflections
2709 independent reflections
1991 reflections with $I > 2\sigma(I)$
R_{int} = 0.028
θ_{max} = 73.0°, θ_{min} = 4.2°
h = −13→15
k = −12→12
l = −15→14

Refinement

Refinement on F^2
Least-squares matrix: full
$R[F^2 > 2\sigma(F^2)]$ = 0.046
$wR(F^2)$ = 0.142
S = 1.03
2709 reflections
169 parameters
1 restraint
Hydrogen site location: mixed
H atoms treated by a mixture of independent and constrained refinement
$w = 1/[\sigma^2(F_o^2) + (0.0713P)^2 + 0.2035P]$ where $P = (F_o^2 + 2F_c^2)/3$
$(\Delta/\sigma)_{max} < 0.001$
$\Delta\rho_{max}$ = 0.15 e Å^{-3}
$\Delta\rho_{min}$ = −0.18 e Å^{-3}

Special details

Geometry. All esds (except the esd in the dihedral angle between two l.s. planes) are estimated using the full covariance matrix. The cell esds are taken into account individually in the estimation of esds in distances, angles and torsion angles; correlations between esds in cell parameters are only used when they are defined by crystal symmetry. An approximate (isotropic) treatment of cell esds is used for estimating esds involving l.s. planes.

Refinement. Single-crystal X-ray diffraction data were collected on an Agilent SuperNova Dual Atlas diffractometer, equipped with a mirror monochromator and using Mo radiation. The data were processed using CrysAlisPro (Rigaku OD, 2024) and the crystal structures were solved using SHELXT(Sheldrick, 2015a) and refined using SHELXL(Sheldrick, 2015b). Non-hydrogen atoms were refined with anisotropic displacement parameters.

Fractional atomic coordinates and isotropic or equivalent isotropic displacement parameters (Å²)

	x	*y*	*z*	U_{iso}*/U_{eq}
C1	0.59743 (15)	0.60953 (13)	0.71939 (15)	0.0484 (4)
C2	0.51238 (15)	0.65227 (14)	0.59945 (16)	0.0515 (4)
C3	0.38984 (18)	0.67279 (17)	0.5722 (2)	0.0661 (5)
H3	0.332387	0.701082	0.493473	0.079*
C4	0.3519 (2)	0.6523 (2)	0.6586 (2)	0.0799 (6)
H4	0.269123	0.665369	0.638096	0.096*
C5	0.4366 (2)	0.6123 (2)	0.7762 (2)	0.0776 (6)
H5	0.409988	0.599209	0.834640	0.093*
C6	0.56176 (18)	0.59086 (16)	0.80978 (18)	0.0601 (4)
C7	0.55179 (17)	0.67607 (17)	0.50351 (16)	0.0627 (5)
H7A	0.615717	0.740284	0.532914	0.094*
H7B	0.481579	0.704990	0.428263	0.094*
H7C	0.583419	0.598230	0.487688	0.094*
C8	0.6532 (2)	0.5506 (2)	0.94016 (19)	0.0789 (6)
H8A	0.623068	0.576806	0.995803	0.118*
H8B	0.732437	0.590077	0.964372	0.118*
H8C	0.662476	0.459214	0.943309	0.118*
C9	0.77763 (16)	0.47292 (15)	0.76710 (16)	0.0552 (4)
C10	0.90876 (18)	0.47159 (18)	0.7846 (2)	0.0701 (5)
H10A	0.967251	0.474147	0.872751	0.084*
H10B	0.921820	0.391831	0.752147	0.084*
C11	1.06707 (17)	0.6107 (2)	0.77925 (19)	0.0723 (6)
H11A	1.113068	0.540388	0.768972	0.087*
H11B	1.100787	0.626798	0.867333	0.087*
C12	1.0799 (2)	0.7277 (3)	0.7164 (3)	0.0927 (7)
H12A	1.033815	0.797529	0.727217	0.111*
H12B	1.166922	0.752477	0.754614	0.111*
C13	0.9087 (2)	0.6687 (3)	0.5317 (2)	0.0856 (7)
H13A	0.879929	0.650423	0.444758	0.103*
H13B	0.859282	0.738908	0.536367	0.103*
C14	0.88885 (18)	0.55288 (19)	0.59218 (18)	0.0681 (5)
H14A	0.800777	0.532485	0.552940	0.082*
H14B	0.932346	0.480240	0.581836	0.082*
N1	0.72330 (13)	0.58889 (13)	0.74639 (13)	0.0509 (3)
N2	0.93530 (13)	0.57730 (13)	0.72435 (13)	0.0560 (4)

O1	0.72824 (12)	0.37440 (11)	0.77594 (13)	0.0708 (4)
O2	1.03491 (16)	0.70609 (19)	0.58815 (17)	0.0980 (5)
H1	0.7656 (17)	0.651 (2)	0.7350 (17)	0.063 (5)*

Atomic displacement parameters (Å²)

	U^{11}	U^{22}	U^{33}	U^{12}	U^{13}	U^{23}
C1	0.0522 (9)	0.0332 (7)	0.0626 (10)	−0.0040 (6)	0.0298 (8)	−0.0032 (6)
C2	0.0541 (9)	0.0345 (7)	0.0616 (10)	−0.0016 (6)	0.0244 (8)	−0.0046 (6)
C3	0.0557 (11)	0.0564 (10)	0.0773 (12)	0.0046 (8)	0.0247 (9)	−0.0071 (9)
C4	0.0616 (12)	0.0824 (14)	0.0993 (16)	0.0035 (10)	0.0415 (12)	−0.0113 (12)
C5	0.0845 (14)	0.0762 (13)	0.0971 (15)	−0.0076 (11)	0.0636 (13)	−0.0083 (11)
C6	0.0716 (11)	0.0480 (8)	0.0692 (11)	−0.0065 (8)	0.0405 (9)	−0.0021 (7)
C7	0.0663 (11)	0.0556 (9)	0.0587 (10)	−0.0013 (8)	0.0240 (9)	0.0031 (8)
C8	0.1016 (16)	0.0738 (13)	0.0672 (12)	−0.0096 (11)	0.0454 (12)	0.0046 (10)
C9	0.0610 (10)	0.0412 (8)	0.0593 (9)	0.0059 (7)	0.0256 (8)	0.0059 (7)
C10	0.0655 (11)	0.0585 (10)	0.0839 (13)	0.0172 (9)	0.0340 (10)	0.0170 (9)
C11	0.0520 (10)	0.0900 (14)	0.0732 (12)	0.0018 (10)	0.0286 (9)	−0.0206 (10)
C12	0.0801 (15)	0.1038 (18)	0.1115 (19)	−0.0305 (13)	0.0599 (14)	−0.0280 (15)
C13	0.0780 (15)	0.1089 (18)	0.0800 (14)	0.0046 (12)	0.0459 (12)	0.0102 (12)
C14	0.0577 (11)	0.0731 (12)	0.0684 (11)	0.0027 (9)	0.0261 (9)	−0.0114 (9)
N1	0.0518 (8)	0.0385 (6)	0.0625 (8)	0.0000 (6)	0.0274 (7)	0.0047 (6)
N2	0.0500 (8)	0.0539 (8)	0.0638 (9)	0.0054 (6)	0.0270 (7)	−0.0005 (6)
O1	0.0787 (9)	0.0401 (6)	0.0902 (9)	0.0026 (6)	0.0376 (7)	0.0090 (6)
O2	0.0848 (11)	0.1313 (15)	0.1008 (12)	−0.0166 (10)	0.0629 (10)	−0.0041 (10)

Geometric parameters (Å, º)

C1—C6	1.388 (2)	C9—C10	1.514 (3)
C1—C2	1.408 (2)	C10—N2	1.451 (2)
C1—N1	1.428 (2)	C10—H10A	0.9700
C2—C3	1.388 (2)	C10—H10B	0.9700
C2—C7	1.493 (2)	C11—N2	1.461 (2)
C3—C4	1.363 (3)	C11—C12	1.495 (3)
C3—H3	0.9300	C11—H11A	0.9700
C4—C5	1.378 (3)	C11—H11B	0.9700
C4—H4	0.9300	C12—O2	1.415 (3)
C5—C6	1.400 (3)	C12—H12A	0.9700
C5—H5	0.9300	C12—H12B	0.9700
C6—C8	1.508 (3)	C13—O2	1.412 (3)
C7—H7A	0.9600	C13—C14	1.499 (3)
C7—H7B	0.9600	C13—H13A	0.9700
C7—H7C	0.9600	C13—H13B	0.9700
C8—H8A	0.9600	C14—N2	1.462 (2)
C8—H8B	0.9600	C14—H14A	0.9700
C8—H8C	0.9600	C14—H14B	0.9700
C9—O1	1.225 (2)	N1—H1	0.88 (2)
C9—N1	1.347 (2)		

C6—C1—C2	121.55 (16)	C9—C10—H10A	108.8
C6—C1—N1	120.77 (15)	N2—C10—H10B	108.8
C2—C1—N1	117.65 (15)	C9—C10—H10B	108.8
C3—C2—C1	118.14 (17)	H10A—C10—H10B	107.7
C3—C2—C7	120.37 (16)	N2—C11—C12	108.90 (17)
C1—C2—C7	121.48 (15)	N2—C11—H11A	109.9
C4—C3—C2	121.4 (2)	C12—C11—H11A	109.9
C4—C3—H3	119.3	N2—C11—H11B	109.9
C2—C3—H3	119.3	C12—C11—H11B	109.9
C3—C4—C5	119.9 (2)	H11A—C11—H11B	108.3
C3—C4—H4	120.1	O2—C12—C11	111.30 (19)
C5—C4—H4	120.1	O2—C12—H12A	109.4
C4—C5—C6	121.5 (2)	C11—C12—H12A	109.4
C4—C5—H5	119.2	O2—C12—H12B	109.4
C6—C5—H5	119.2	C11—C12—H12B	109.4
C1—C6—C5	117.51 (18)	H12A—C12—H12B	108.0
C1—C6—C8	122.04 (17)	O2—C13—C14	112.33 (19)
C5—C6—C8	120.45 (18)	O2—C13—H13A	109.1
C2—C7—H7A	109.5	C14—C13—H13A	109.1
C2—C7—H7B	109.5	O2—C13—H13B	109.1
H7A—C7—H7B	109.5	C14—C13—H13B	109.1
C2—C7—H7C	109.5	H13A—C13—H13B	107.9
H7A—C7—H7C	109.5	N2—C14—C13	109.88 (17)
H7B—C7—H7C	109.5	N2—C14—H14A	109.7
C6—C8—H8A	109.5	C13—C14—H14A	109.7
C6—C8—H8B	109.5	N2—C14—H14B	109.7
H8A—C8—H8B	109.5	C13—C14—H14B	109.7
C6—C8—H8C	109.5	H14A—C14—H14B	108.2
H8A—C8—H8C	109.5	C9—N1—C1	124.03 (14)
H8B—C8—H8C	109.5	C9—N1—H1	114.7 (12)
O1—C9—N1	123.59 (16)	C1—N1—H1	120.2 (12)
O1—C9—C10	120.97 (15)	C10—N2—C11	114.49 (15)
N1—C9—C10	115.40 (14)	C10—N2—C14	111.77 (15)
N2—C10—C9	113.74 (14)	C11—N2—C14	107.98 (14)
N2—C10—H10A	108.8	C13—O2—C12	109.88 (16)
N1—C9—C10—N2	−26.1 (2)		

Hydrogen-bond geometry (Å, º)

*Cg*2 is the centroid of the C1–C6 ring.

D—H···*A*	*D*—H	H···*A*	*D*···*A*	*D*—H···*A*
N1—H1···N2	0.88 (2)	2.278 (18)	2.738 (2)	112.5 (16)
N1—H1···O1^{i}	0.88 (2)	2.34 (2)	3.0798 (18)	141.3 (16)
C10—H10*B*···*Cg*2^{ii}	0.97	2.94	3.782 (2)	146

Symmetry codes: (i) −*x*+3/2, *y*+1/2, −*z*+3/2; (ii) −*x*+3/2, *y*−1/2, −*z*+3/2.